Revista GEOSABERES

www.geosaberes.ufc.br
ISSN: 2178-0463

PETROLOGY AND PETROGENESIS OF SIAH KOOH VOLCANIC ROCKS IN THE EASTERN ALBORZ

PETROLOGIA E PETROGÊNESE DAS ROCHAS VULCÂNICAS SIAH KOOH, EM ALBORZ ORIENTAL

PETROLOGÍA Y PETROGÉNESIS DE LAS ROCAS VOLCÁNICAS DE SIAH KOOH EN EL ALBORZ ORIENTAL

https://doi.org/10.26895/geosaberes.v11i0.980

MOSTAFA BARATIAN [1]
MOHAMMAD ALI ARIAN [2*]
ABDOLLAH YAZDI [3]

[1] PhD Candidate of Petrology, Department of Geology, North Tehran Branch, Islamic Azad University, Tehran, Iran. CP: 4917746846, Tel.: (+98) 9113751973, mostafabaratyan@gmail.com, http://orcid.org/0000-0002-0909-4301.

[2] Associate Professor, Department of Geology, North Tehran Branch, Islamic Azad University, Tehran, Iran. CP: 195991558, Tel.: (+98) 9123788378, maa1361@yahoo.com, http://orcid.org/0000-0001-8193-0274.
* Corresponding Author

[3] Assistant Professor, Department of Geology, Kahnooj Branch, Islamic Azad University, Kahnooj, Iran. CP: 1738633467, Tel.:(+98)9123348430, yazdi_mt@yahoo.com, http://orcid.org/0000-0002-6096-4739.

Article History:
Received 14 January, 2020.
Acepted 11 February, 2020.
Published 18 May, 2020.

ABSTRACT

Siah Kooh area is northeast of Shahroud city and is located in eastern Alborz. The lithologic composition of the volcanic rocks in the area consists of andesite, basalt, trachyandesite and quartztrachite. Plagioclase, olivine, and augite phenocrysts as the main minerals and apatite and magnetite, sericite, chlorite and apacite minerals are sub-minerals of volcanic rocks that are located in the glass slabs. Quartz is also found in fine-grained rock pulp and sometimes in phenocrysts. The dominant texture in these rocks are porphyritic, amygdaloidal and microlithic. According to geochemical studies of basaltic magmatic volcanic rocks, calc-alkaline potassium is high and negative Nb anomaly, Ce / Pb ratio and enrichment of rocks of light rare earth elements (LRRE) and high LREE / HREE ratio indicate contamination. The crust is an indicator of the presence of the garnet phase in the mantle source. On the other hand, the similarity of their trace elements to Oceanic Basalts (OIB) is a clear evidence of their relevance to this environment. Early basaltic magma originated from a mantle with a garnet-lherzolite composition with a partial melting rate of 15–12%. FeOtotal values in basalts and other structural evidence indicate the formation of these rocks in the early stages of intra-continental rifting which can be attributed to the pressure drop caused by intra-continental tidal phases associated with deep faults during the orogenic phases. Alpine attributed to Eocene time.
Keywords: Basalt. Andesite. Tensile environment. Siah Kooh. Iran.

RESUMO

A área de Siah Kooh fica a nordeste da cidade de Shahroud e está localizada no leste de Alborz. A composição litológica das rochas vulcânicas na área é composta por andesita, basalto, traquiandesita e quartztracita. Fenocristais de plagioclásio, olivina e augita como principais minerais e minerais de apatita e magnetita, sericita, clorita e apacita são sub-minerais de rochas vulcânicas localizadas nas placas de vidro. O quartzo também é encontrado na polpa de rocha de grão fino e, às

vezes, nos fenocristais. A textura dominante nessas rochas é porfirítica, amigdaloidal e microlítica. De acordo com estudos geoquímicos de rochas vulcânicas magmáticas basálticas, o potássio cálcio-alcalino é uma anomalia Nb alta e negativa, a relação Ce / Pb e o enriquecimento de rochas de elementos leves de terras raras (LRRE) e a alta relação LREE / HREE indicam contaminação. A crosta é um indicador da presença da fase granada na fonte do manto. Por outro lado, a semelhança de seus oligoelementos com os Oceanic Basalts (OIB) é uma evidência clara de sua relevância para esse ambiente. O magma basáltico inicial se originou de um manto com uma composição granada -herzolita com uma taxa de fusão parcial de 15 a 12%. Os valores totais de FeO em basaltos e outras evidências estruturais indicam a formação dessas rochas nos estágios iniciais da fenda intra-continental, que podem ser atribuídas à queda de pressão causada pelas fases de maré intra-continentais associadas a falhas profundas durante as fases orogênicas. Alpino atribuído ao tempo Eoceno.
Palavras-chave: Basalto. Andesita. Ambiente elástico. Siah Kooh. Irã.

RESUMEN

El área de Siah Kooh está al noreste de la ciudad de Shahroud y está ubicada en el este de Alborz. La composición litológica de las rocas volcánicas en el área consiste en andesita, basalto, traquiandesita y cuarztraquita. Los fenocristales de plagioclasa, olivina y augita como minerales principales y los minerales apatita y magnetita, sericita, clorita y apacita son subminerales de rocas volcánicas que se encuentran en las losas de vidrio. El cuarzo también se encuentra en la pulpa de roca de grano fino y, a veces, en fenocristales. La textura dominante en estas rocas es porfirítica, amigdaloidal y microlítica. De acuerdo con estudios geoquímicos de rocas volcánicas magmáticas basálticas, el potasio alcalino-calcico es una anomalía de Nb alta y negativa, una relación Ce / Pb y el enriquecimiento de rocas de elementos ligeros de tierras raras (LRRE) y una alta relación LREE / HREE indican contaminación. La corteza es un indicador de la presencia de la fase granate en la fuente del manto. Por otro lado, la similitud de sus oligoelementos con los basaltos oceánicos (OIB) es una clara evidencia de su relevancia para este entorno. El magma basáltico temprano se originó a partir de un manto con una composición de granate-lherzolita con una tasa de fusión parcial del 15-12%. Los valores totales en los basaltos y otras evidencias estructurales indican la formación de estas rocas en las primeras etapas de la ruptura intracontinental, lo que puede atribuirse a la caída de presión causada por las fases de marea intracontinentales asociadas con fallas profundas durante las fases orogénicas. Alpine atribuido al tiempo del Eoceno.
Palabras clave: Basalto. Andesita. Ambiente de tracción. Siah Kooh. Irán.

INTRODUCTION

Alborzbeh Mountains as part of the Alpine-Himalayan orogenic belt with a thickness of 35 to 40 km (Guest et al., 2007) from the north to the Caspian block (Zoneshian & Guest et al., 2007) and from the south to the Tabriz-Bazman magmatic arc. And the Iranian block is limited (Guest et al., 2007).

This belt extends from Turkey to Thailand and is divided into three parts from the tectonic point of the Alborz Mountains: West Alborz, Central Alborz and East Alborz. Along the Alps-Himalaya Belt, the western Alborz on the west flows to the Molasses Oligocene to Quaternary Basin in the Kura Basin (Zanchi et al., 2006) and also to the Trans-Caucasian Molasse Basin in northeast Turkey and the eastern part of the Molasse Basin of the Molasses Caucasus Basin (Ershovet al., 2003; Dabiri et al., 2018 ;Yazdi et al., 2019). After the Late Cretaceous compressional phase, a significant extensional phase throughout Iran except for Zagros and Kopet Dagh (which resulted in severe volcanism and Eocene plutonism in most parts of Alborz Azerbaijan) has been investigated in the present study. Relationship between different rock units and geochemical properties and magmatic series and tectonic position of the rocks with modeling to identify the types of processes involved in lithological variability of the area.

DISCUSSION

GENERAL GEOLOGY

The study area is located in eastern Alborz Structure Zone which is located in Semnan province in terms of national divisions (Figure 1). The area lies between the eastern longitude '09 55و and '15 ^{0}55 and the northern latitude '37 ^{0}36 and '33 ^{0}36. The earliest identified

Cenozoic outcrops in this area include plaster marl, red plaster, light plaster green marl between sandstones. Outcrops of rock units in the Eocene period include a thickness of dark volcanic rocks with andesite composition, basalt with andesitic tuffs and green tuffs. The related faults in the Siah Kooh region, which generally trend southwest-northeast and are of the type of trust, can be Dino, Zarrin Kamar and Gachbon faults. The folds of the study area consist mainly of anticline and syncline buildings, the most important of which are the Dino anticline and the Shirin Cheshmeh syncline (Figure 2).

Figure 1- Location of study area (the red circle) from (Aziz et al., 2018) modified from map (Stocklin, 1968)

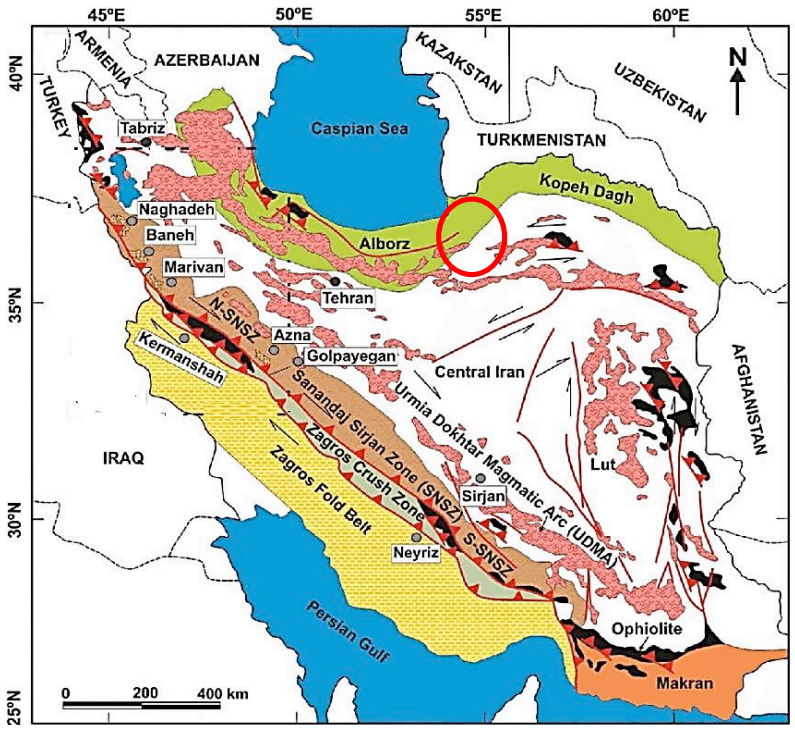

Figure 2 - Location of Siah Kooh region on a map of 1: 100000 Khosh Yeylagh map (Black Sea and 2004).

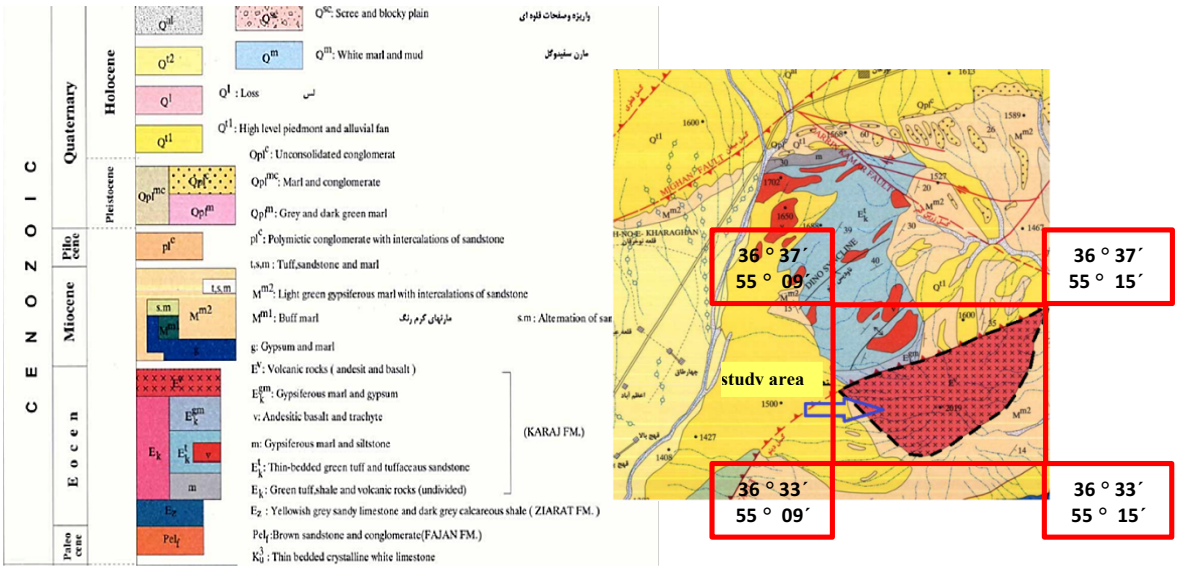

STUDY METHOD

The current research is based on field studies, thin section studies and chemical analysis of the major and trace elements. In this respect more than 25 samples Thin sections have been sampled and studied from the Siah Kooh volcanic rocks. 7 of these XRF and ICP-MS chemical analysis of the major and trace elements was performed at the S. G. S Laboratory, Canada (Table 1).

Table 1- Coordinates of volcanic samples taken from the Black Mountain area

Row	S.N	Latitude	Longitude
1	B36	36° 36' 06.6"	55° 11' 39.9"
2	B41	36° 35' 49.9"	55° 11' 28.4"
3	B50	36° 35' 48.9"	55° 12' 16.5"
4	B64	36° 36' 24.8"	55° 12' 38.3"
5	M42	36° 36' 35.6"	55° 14' 33.1"
6	M44	36° 36' 32.5"	55° 14' 27.8"
7	M50	36° 34' 30.1"	55° 11' 16.7"

LITHOLOGICAL EXAMINATION

Based on the studied samples, the composite spectrum of the studied volcanic rocks is basalt, andesite, trachyte (Figure 3). Detailed petrographic studies on volcanic rocks in the area are as follows:

Basalt B41: Basalts in the dark gray hand sample are predominantly microlytic, porphyric, and amygdaloidal. They include plagioclase, clinopyroxene (oligite) and olivine phenocrysts. Plagioclase crystals are small to medium in size, often automorphic and subatomorphic, elongated and rectangular, with polynthetic, Carlsbad, and sometimes marginally elongated and sometimes albite margins.

Conjugation of plagioclase crystallization with pyroxene crystals is seen in some specimens that sometimes form along the biotite crystals and sometimes become thermolithic. The olivine crystals are small in size, often subamorphic and have been altered to biotite, serpentine, chlorite and iron oxide. The pulp consists of glass, plagioclase microliths, OPAC minerals, and secondary minerals. OPAC minerals are by-products of these rocks. The cavities (common and camel-shaped) are often filled with calcite (Figure. 3a and b). Andesite B64: The andesite rocks are seen in the hand sample, from gray to light brown. The texture of these rocks is mainly porphyritic with microlithic pulp and in some cases porphyritic with microcrystalline and sieve pulp (Figure. 3c). Plagioclase and clinopyroxene phenocrysts are found in very fine areas including plagioclase, clinopyroxene crystals, OPAC and glass minerals (Figure. 3d). Plagioclases are flat, elongated and long and often have a complete shape and their frequency is 85-70%. Sometimes they are very large with polysynthetic molecules. Two plagioclase types were identified with simple and polysynthetic macaques. Types of simple Twining are generally Fracture and crushed. Iron-bearing opaque minerals are angular, tall, and scattered. Olivine is dark green to yellow in shape. Chlorite and cericite were identified as secondary minerals in the samples. Sieve texture is visible in the specimens as a result of the presence of pyroxene and glass inclusions in plagioclase or hybrid imbalance. (Figure. 3d, e). B36 trachea andesite: This rock unit is gray in macroscopic view. Examples of the area are flow and trachyte structures. Porphyritic texture with microlithic pulp and trachytic texture. Contains plagioclase and pyroxene phenocrysts in the microlithic

paste often of plagioclase. Plagioclase phenocrysts are gray and almost full-bodied, sometimes very coarse-grained and elongate, with long, flat-shaped, slightly semi-shaped boards between thin and dense blades of feldspars. The polysynthetic twinning are clearly shown. In some cases, the blades are uniform and uniform in size, and in some cases large, flowing. The intersections are intersections. They have polycynthetic compositional zones and polysynthetic motifs (Figure -3, h) and some contain apatite editions. In some instances, the blades are identical and the same size, and in some cases are slightly larger and flowing. They are intersected at points in sections.

Figure 3: a- Porphyritic texture with microlith glass paste, plagioclase phenocrysts and pyroxenes in basalt (XPL). b- Porphyritic texture with glassy and pithy pulp, plagioclase and pyroxene phenocrysts in basalt (XPL). C- Puffiritic texture with glassy and microlithic pulp, plagioclase and epidote mineralization in andesite (XPL). d and e - Puffyrite texture with glassy to microlithic glass pulp, sieve texture of plagioclase crystals in andesite (XPL). e. Conversion of plagioclase and its replacement with chlorite and OPAC mineralization in andesite (XPL). g- andesite rocky-flow (XPL). h- Porphyritic texture with microlithic pulp and cavity in trachy andesite filled with secondary chlorite (section 36). Porphyritic texture with glass pulp with plagioclase, alkali feldspar, quartz and OPAC mineralization in trachyte (XPL and PPL).

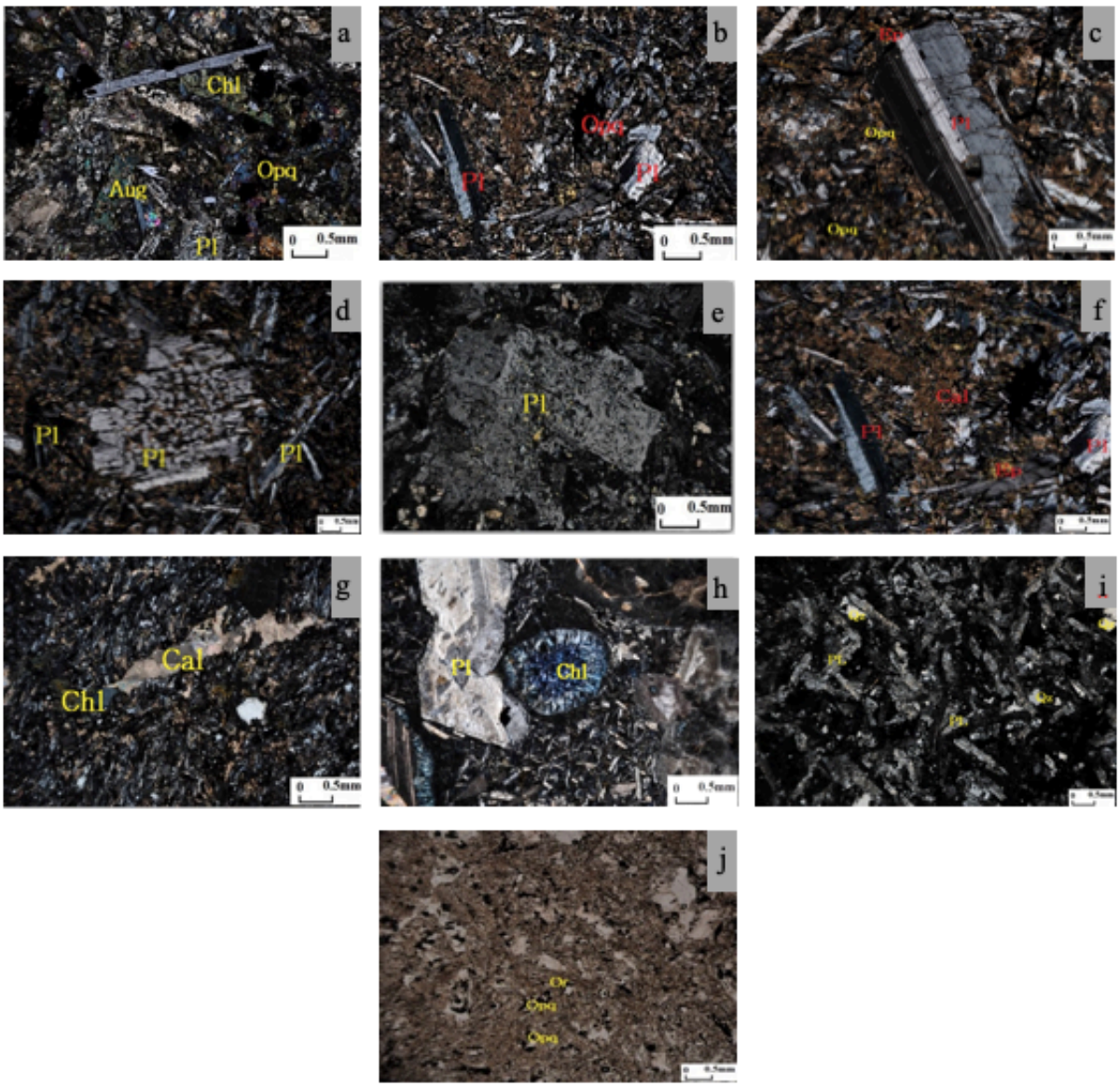

They have compositional zones and polysynthetic twinning (Figure-3, h) and some contain apatite editions. Plagioclases have been altered to cericite and clay minerals, giving a dusty appearance. The pyroxene phenocryst, one of the common minerals in this rock, is found to form crystalline to amorphous crystals and is often fractured. The color of these crystals is colorless, occasionally pale green, yellow and pink (due to the presence of Ti), with transverse sections having two distinct facies, high prominence and extinction angle of about 45 degrees. Therefore, due to the microscopic properties of these crystals, they are clinopyroxene (augite type). The opaque minerals magnetite and titanomagnetite are dark and black to red, often Interference, sometimes dispersed and angular to semi-shaped, and are the most abundant OPAC sub-minerals in andesite. Olivine and magnetite microliths are dispersed in the dough. Apatite is also present in small amounts in small crystals, within the plagioclase and rarely in the dough. The presence of fine-grained apatite in phenocrysts indicates early crystallization of this mineral. The most important secondary minerals are chlorite and sericite (as a result of pyroxene and plagioclase alteration), calcite and biotite (Figure 3-g). Quartz are very fine-grained and are located between mineral intervals and their abundance is 10% to 5%. The round, elliptical cavities of the gas outflow are filled by secondary minerals such as calcite and quartz. Quartztracite M42: This rock unit, seen in small dikes and floods, is gray in macroscopic view. (Figure 3 i,j). Porphyric texture of the amygdala with all-crystalline pulp. Phenocrysts are of potassium, biotite or amphibole feldspars and rarely pyroxene, and the minerals that make up the rock are usually potassium feldspars, plagioclase, amphibole, alkaline pyroxenes, and quartz-like and semi-crystalline fine-grained to semi-crystalline forms Feldspars, formed. At this point, large, elongated feldspar phenocrysts are clayey, shale-shaped, and sometimes semicircular in color to gray to light brown in color and sometimes chlorite. Among these feldspars there are circular, spherical and elliptical gaps in the gas outflow that fill the secondary minerals such as calcite, quartz and chlorite secondary minerals, calcite, magnetite. In the meantime, the coniferous minerals are light green, light brown to shapeless, regular and dispersed at the cross-section. The metallic opacite minerals are scattered, shapeless to semicircular and angular in the text. Most plagioclases are decomposed into sericite, chlorite, clay minerals. Quartz is also seen as granulocytes in rock pulp and sometimes as phenocrysts. Minerals in the andesitic rocks of the area can be mentioned as opaque and apatite.

GEOCHEMISTRY

For naming the units, determining the crystallization conditions of the magma and melting processes after studying the thin sections, 7 samples were selected and sent to SGS Canada after crushing and preparation of rock samples taken from the area for geochemical determination of the samples by ICP method. Was. Seven samples were also sent to Zarazma for ICP and ICP analysis. SiO2 content in these rocks varied from 37.81% in basalts to 65.62% in quartztracite, with Al_2O_3% and MgO up to 7%, total iron oxide up to 14.6%, Sodium and Potassium oxides separately up to 7%. The percentage reaches. Calcium oxide also has a wide range and a high percentage from 0.5% to 16%. According to the TAS diagram these rocks are located in the composite ranges of basalt, rhyolite, trachyte and trachy andesite (Figure. 4a). Based on the segmentation boundary of the semi-alkaline and alkaline series (Irvine & Baragar, 1971), the magmas forming the rocks under study show the calc-alkaline nature (Figure. 4b). In the Th-Co diagram (Hastie et al., 2007) these rocks are in the range of calc-alkaline to high-potassium calc-alkaline (Shoshoniite) (Figure 4c). In the diagram (FeO + MgO) vs. SiO_2 (Schrader 2001) (Figure. 4d), located on the SiO_2 axis of the feldspar and feldsparoid compounds, all the samples are in descending order, and did they have the black samples tend to be alkali feldspar, nepheline and plagioclase And this can be justified by the study of microscopic thin sections. In order to study the crystallization process

and processes governing the development of magma and also considering the basic of the studied samples, the process of changes of some major and minor element oxides against MgO (Fenner diagrams) has been studied (Figure. 5). As can be seen, the amount of MgO changes in all samples varied between 0.5% and 8%, and due to the accumulation in this range, significant trends were observed. The two inactive P and Ti elements show an increasing trend as the amount of MgO decreases. Based on petrographic evidence of apatite presence in the rocks of the region and incompatibility of P with the composition of the main minerals of the rocks in the region, the concentration of this element in the volcanic glass should be considered. The increasing trend of TiO_2, coupled with the increasing trend of MgO, confirms the petrographic evidence for the initial crystallization of titanium oxides (as OPAC phases) in the rocks of the region.

Figure 4: Diagram of $Na_2O + K_2O$ vs. SiO_2 (Cox et al., 1979) B- Irvine and Baragar magmatic series diagrams, (1971) c. Tholeiitic and calc-alkaline ranges and location of samples in the region. Basalt: B, Basalt-Andesite: BA / A and Dacite and Rhyolite: D / R D - Graph of changes in total elemental elements (FeO + MgO relative to SiO_2 Schrader 2001) for volcanic rocks in the region.

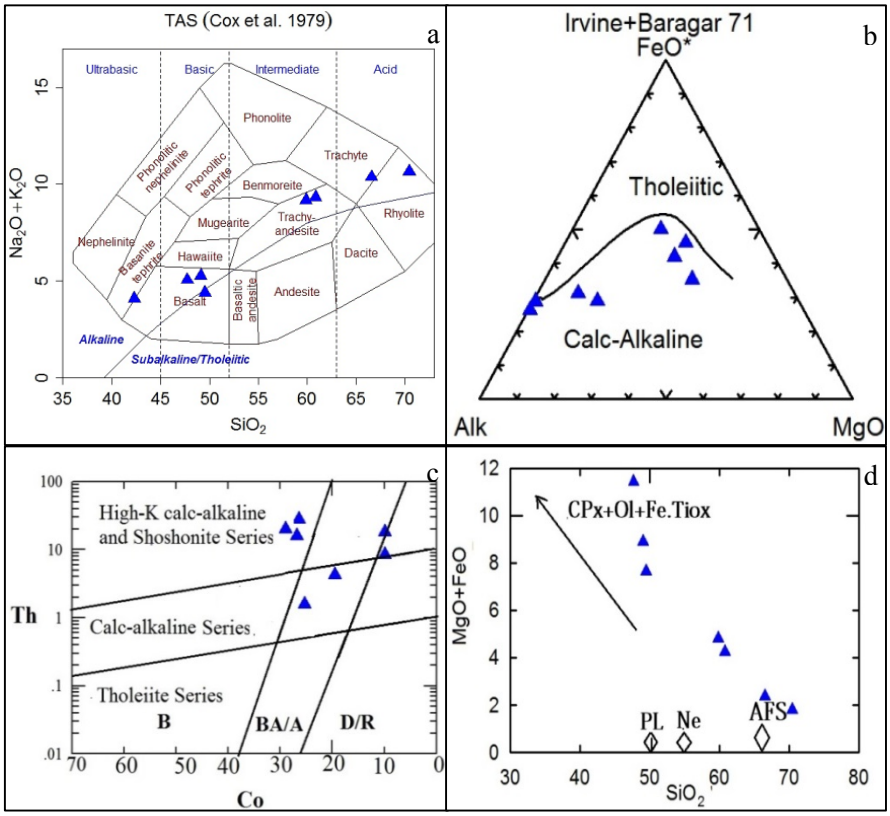

In the graph of changes of Fe_2O_3 versus MgO, the amount of Fe_2O_3 decreases with decreasing MgO and increasing subtraction. The graph shows that more subtracted samples have less iron. This trend indicates that in the early stages of subtraction, MgO and Fe levels were also high, so that with increasing magma subtraction, the more subtracted fraction would have less FeO. The decreasing trend of Al_2O_3 and SiO_2 against MgO implies that the crystallization of olivine precedes partial crystallization of plagioclase in the liquid phase. The decreasing trend of K_2O and Na_2O against MgO also indicates partial crystallization of magma and partly their dispersion is the result of partial alteration or contamination with felsic crustal material. The increase in MgO with CaO and Fe_2O_3(T) indicates the importance

of crystallization of pyroxenes in the rocks present in the region (Gouragaud & Vincent, 2003; Arfania 2018; Ashrafi et al., 2018) and both show similar trends.

Figure 5 - Trends of Oxides of Main Elements vs. MgO

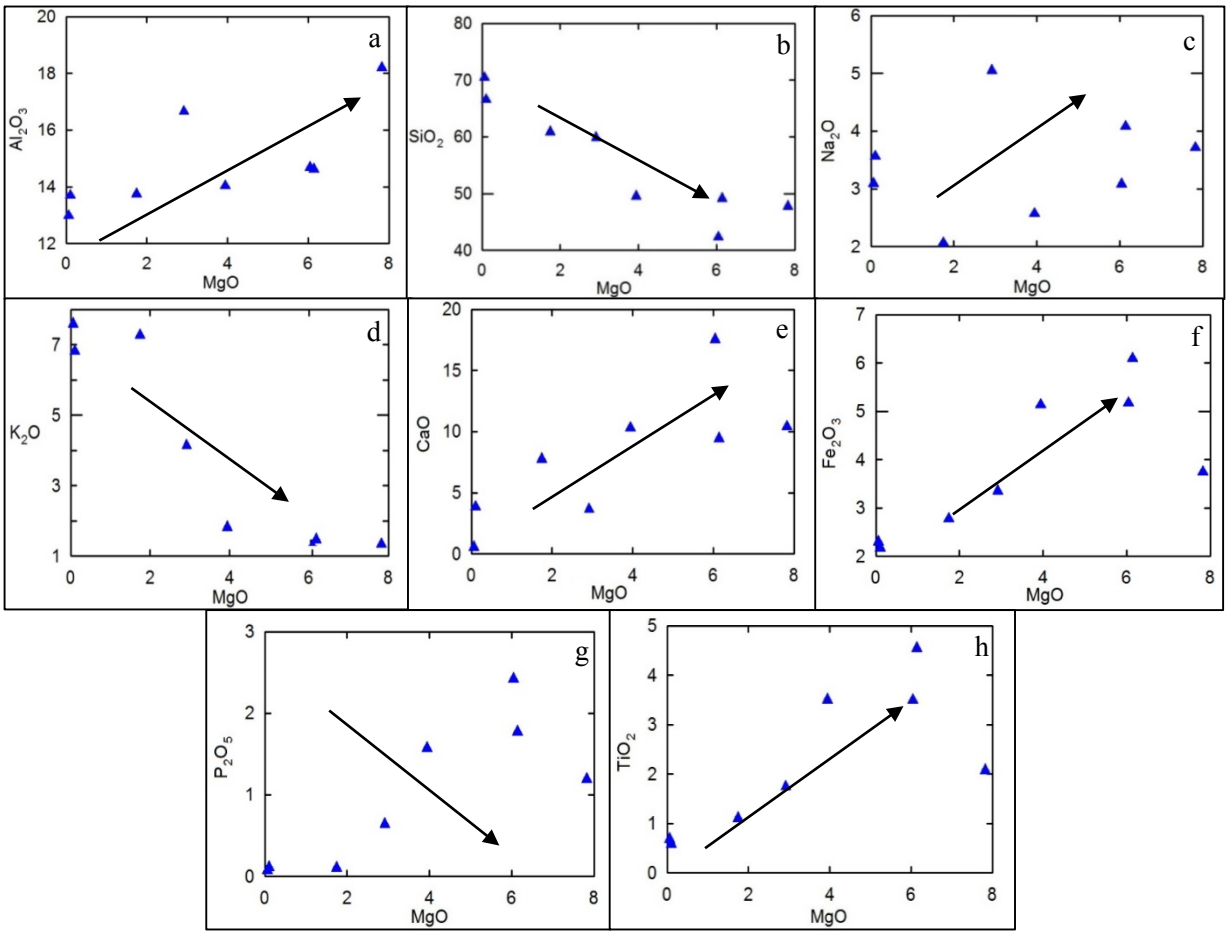

In the following, the process of changing the highly compatible elements Ni, Nb, Co, Ce versus the highly incompatible element Zr is discussed (Figure. 6). Zr is completely incompatible with geochemical behavior during partial melting and subduction in basaltic melt (Talusami, 2010) and is highly inclined to enter and remain in the molten phase. Very low mobility of this element during alteration as well as the range of extensive changes of this element in basaltic rocks (Le Roex et al., 1983; Mitchell & Tatsumi et al., 1986; Meng, 2012; Talusami, 2010; Widdowson et al., 2000 Widdowson, 1991) has also been an additional factor. In Figure (6), the graphs show mostly linear and upward trends that also pass the source of the coordinates. Therefore, according to this model, the dominant process in the magmatic evolution of the region is subduction crystallization.

The general trend of Ni and Co, which are olivine incompatible elements, and their reduction indicate the importance of crystallization of the primary part of the mineral in the basaltic melt. In fact, this mineral is incompatible with Th, but its compatibility with Ni and Co has led to a sharp decrease in these two elements.

Figure 6 (a, b, c and d) - diagrams of changes of compatible and incompatible elements (e)

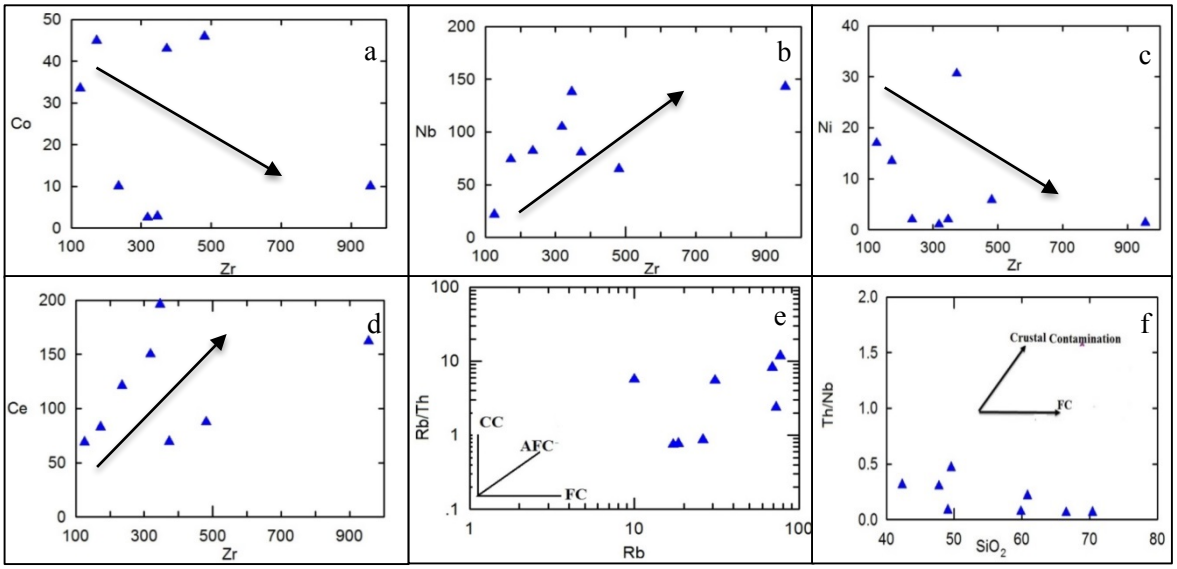

Diagrams of Th / Nb changes against SiO_2 in order to determine the crustal contamination rate and its role in the evolution of magma-forming rocks in the region. Submitted by He et al., (2010) (and) the trends identified in the figure are: CC: shell contamination, AFC: subtraction crystallization with digestion, FC: subtraction crystallization, for Siahkoh volcanic rocks.

The upward trend of the samples in the Rb / Th vs. Rb variation graph (Tchameni et al. 2006) illustrates the role of the subtraction crystallization process (AFC) and contamination by a crustal source in the rocks studied (Figures. 6 and 6).). The trend observed on the Th / Nb change diagram against SiO2 (Figure 7) is further confirmation by He et al., 2010).

Figure 7 – a: Nb vs. Zr diagram (Abu-Hamatteh et al. 2005) b: Zr / Nb vs. Zr / Y The samples studied are in the OIB range c: Pearce & Norry, 1979

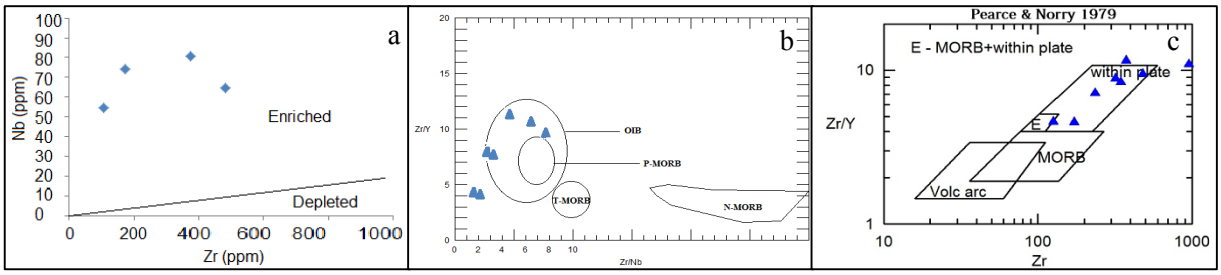

Nb-Zr diagrams (Abu-Hamatteh et al. 2005) were used to detect enrichment or non-enrichment of the source rocks (Figure. 7a). These ratios in the primitive mantle are about Nb / Zr = 15. 71 and Y / Zr = 2.46 (calculated by (Sun and McDonough, 1989)). The source of the enriched mantle has originated.

According to the Pearce & Norry diagram, 1979, Siah Kooh volcanic rocks are formed within the intra-plate boundary (Figure. 7c) and related to the OIB environment (Figure. 7b).

In order to examine more closely the geological processes and characteristics of the source rocks of the region, the normalized and trace elements pattern of these rocks has been standardized to chondrite, primary mantle, diagonal and OIB values (Figure. 8). Normalized diagrams of trace elements relative to chondrite values (Sun and Mc Donough, 1989) for the samples in the study area are almost parallel and only the Eu element can be seen as a

consequence of this. Subtraction of plagioclase and clinopyroxene (Zeng et al., 2010) during the evolution of magma-forming rocks in the region was considered. Negative anomalies in Rb, Nb and P also indicate the role of continental crustal magmatic contamination in the evolution of regional rocks. Severe positive Pb and Ba anomalies indicate continental crustal contamination and Sr positive anomaly indicates the presence of plagioclases in the rock. More than 10-fold enrichment of light trace elements to heavy rare earth elements in most samples indicated a garnet enter the melt and remain in the mantle source. The parallel pattern of distribution of trace elements, their almost constant changes, and the slope of the pattern of distribution of trace elements, are due to the effect of partial crystallization in the development of all kinds of basaltic to middle rocks. The relatively steep HREE / LREE slope in the diagrams is an indication of the presence of a garnet phase in the mantle source, suggesting a deep garnet lherzolite source with phlogopite / paragasite (mantle hornblende) at 2,5.5 gp for alkaline basalts. (Thirlwall et al. 1994; Tappa. 2004; Stivenson, 2003; Glasser et al. 1999). In the normalized Oceanic Basalts (OIB) graph, the observed trend of these samples is approximately equal to and consistent with the OIB values. Given the alkaline nature of these rocks and the similarity of their trace elements to Oceanic Basalts (OIB), these rocks can be identified in relation to these environments (Figure. 8c).

Figure 8 - Rare and rare earth elements from regional rocks normalized to a: chondrite and early mantle values (c: OIB and d: Morbi Pearce, 1983)

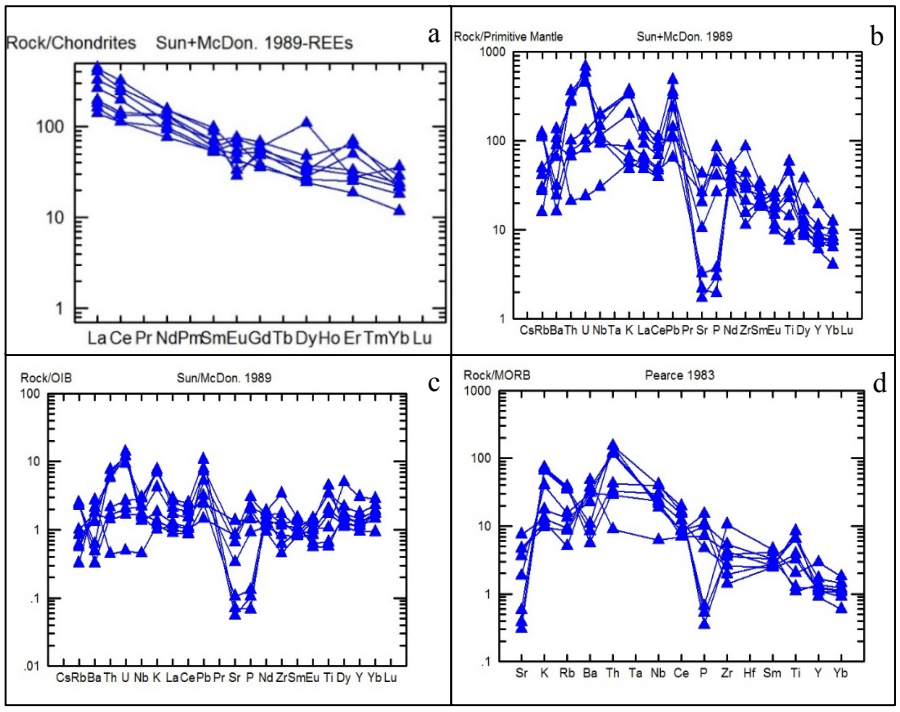

According to the diagrams to determine the tectonic position of the magmatic rocks of the region, the alkaline basalt formation setting of the Black Mountain volcanic rocks are associated with intra-continental or intra-plate rifts (Figure. 9a, b, c).

Figure 9 – a: Chart (Cabanis Lecolle, 1989); b: Chart (Pearce, 1982); c: Biermanns Diagram, 1996, 1. Primary arc island gabbros. 2. Transformed arc island gabbros. 3. Continental arc gabbros. 4. Continental-continental collision gabbros. 5. Intra-continental rift gabbros. Calculate the percentage of partial melting (Aldanmaz et al., 2006) for the Black Mountain volcanic rocks. PM denotes initial mantle and thick lines indicating partial melting curves for mantle origin of spinel lherzolite and garnet lherzolite. The numbers on the curve represent the degrees of partial melting

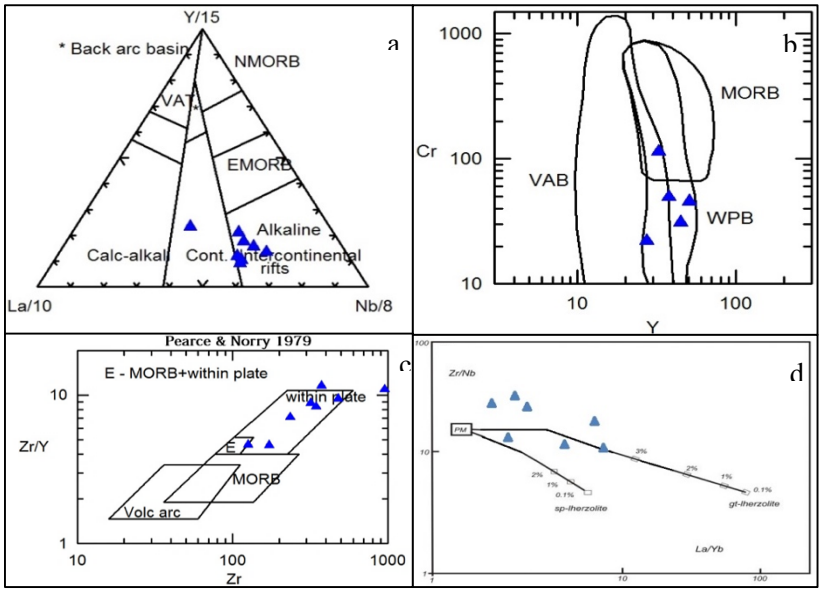

Partial melting curves for spinel lesolorite (Sp11 + Cpx15 + Opx25 + Ol53) and garnet peridotite (Gt10 + Cpx10 + Opx20 + Ol60) as shown in Figure 10 were used to determine the source and melting zone characterization. In both curves, basaltic samples of the area are in the Garnet Lerzolite range. Yb is generally compatible with garnet, while La and Sm are incompatible. This factor causes Sm / Yb and La / Yb to be highly concentrated in garnet peridotite origin during low melting degrees. In contrast, during partial melting in the spinel stability range the La / Yb ratio is only slightly subtracted and the Sm / Yb ratio remains almost unchanged (Xu et al., 2005; Yaxley, 2000; White & Mckenzi, 1995). In the La / Yb diagram against Dy / Yb the samples studied are in the range of 11 to 15% of the garnet peridotite range (Figure 10b).

Figure 10 - a: Sm diagram against Sm / Yb (Green, 2006) b. Dy / Yb vs. La / Yb diagram from Thirlwall et al., (1994) and Bogaard et al., (2003) to determine the degree of melting Part

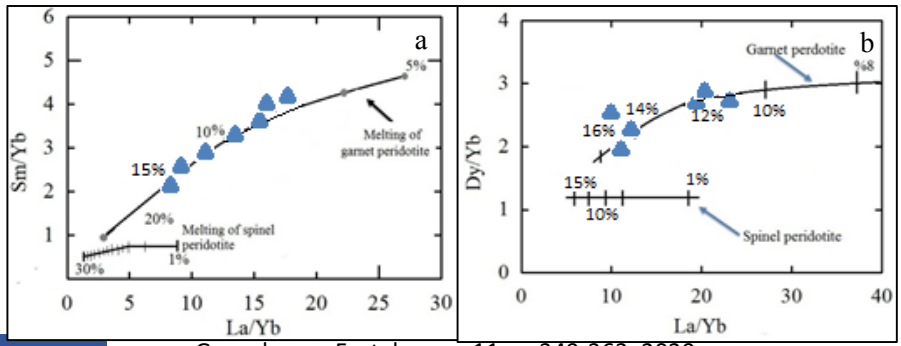

PRESENTING A GEODYNAMIC MODEL FOR THE FORMATION OF IGNEOUS ROCKS IN THE STUDY AREA

Stratigraphic and structural studies (Allen et al., 2003) show that AMA volcanoclastic deposits formed during a tectonic phase in the early Eocene, and Asiabanha and Foden (2012) suggest that this tectonics occurs in an environment The back-arc has occurred.

Due to the basin uplift during the late Eocene compressional regime, the subsequent volcanic phase occurred sub-aerial. Based on the findings and researches, the following model can be presented for Eocene-Oligocene magmatism activity in Alborz and the study area that resembles the Humphreys et al., (2003) model with four stages:

1- In the first stage, the steep subduction of the oceanic crust has resulted in the formation of a volcanic arc or arc in the north of the Arabic-Eurasia Structural Zone.

2- In the second stage after the Aptian-Albian orogenic phase, subduction continued with less slope and caused magmatic activity in north central Iran and Alborz. At the end of the Cretaceous, a series of tectonic contractions occurred in Iran to the north of this structural zone. The upper mantle has also risen in the Alborz Mountains and northern Iran at this stage.

3- This is the Eocene roll back time in the oceanic crust. The reasons for roll back are numerous and depend on the rate of subduction, age of the sheet, the density difference between the sheet and the mantle, etc. (Heuret and Lallemand, 2005). This causes thinning in the crust and elevation of the asthenosphere. Partial melting of hydrated peridotite occurs in the mantle due to reduced pressure and heat. The magma resulting from this melting is depleted of HFSE elements but enriched by some elements during subduction as a result of dehydration performance. At this stage, volcanic activity and shallow marine sediments are formed in extensional environments. The resulting magmas have ascended along the deep faults in the extensional zone and have undergone various petrological processes during the ascent, such as subduction crystallization with crustal digestion and contamination. Existing alkaline magmas were able to erupt as lava in a lake environment and in the formation of red marl sediments (Figure 11).

Figure 11 - Schematic view of the process of formation of alkaline magmas forming Eocene Black Mountain volcanic rocks, inspired by the design (Temizel and Arslan, 2008)

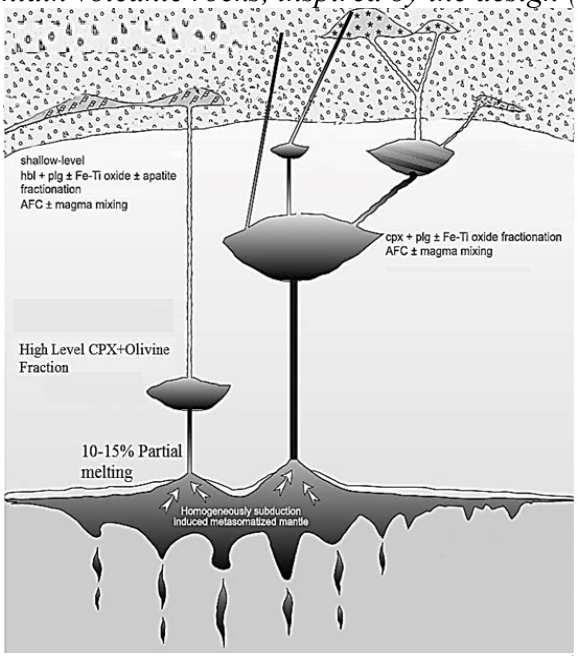

4- At this stage, as the Oligocene began, the asthenospheric uplift occurred due to thinning in the lithosphere. Partial melting in the asthenosphere has led to the formation of basaltic magmas in extensional basins at this time. These basaltic magmas are less polluted due to thinning in the crust and exhibit much of the early magma properties (Plank and Langmuir, 1988; Glazner and Ussler, 1989).

CONCLUSION

According to studies, the rock units of the area consist of basaltic, andesite, trachy andesite and quartztrachite volcanic rocks with alkaline nature. Examination of the normalized diagrams shows that the rocks of the region originate from relatively enriched austenospheric mantle sites similar to the OIB source site with partial melts of 11 to 15 with garnet-laurelite composition. According to tectonic diagrams and structural studies of the Black Mountain rocks are formed in an intra-continental tensile setting.

REFERENCES

ALLEN, M. B., GHASSEMI, M. R., SHAHRABI, M. & QORASHI, M. Accommodation of Late Cenozoic oblique shortening in the Alborz range, northern Iran", 2003. **Journal of Structural Geology** Vol.25. PP., 659-675.

ALLEN, M. B., STEPHEN, J. V., ALSOP, G., ISMAIL ZADEH, A. & FLECKER, R. b-late Cenozoicdeformation in the South Caspian region: effects of a rigid basement block within a collision zone. 2003. **Tectonophysics**, V. 366, P. 223-239.

ARFANIA, Ramin. Role of supra-subduction zone ophiolites in the tectonic evolution of the southeastern Zagros Orogenic Belt, Iran, 2018. **Iranian Journal of Earth Sciences**, 10(1) pp 31-38.

ASHRAFI, Nasser; HASEBE, Noriko; JAHANGIRI, Ahmad. Cooling history and exhumation of the Nepheline Syenites, NW Iran: Constraints from Apatite fission track, 2018. **Iranian Journal of Earth Sciences**, 10(2) pp 109-120.

ASIABANHA, A.; FODEN, F. Post-collisional transition from an extensional volcano-sedimentary basin to a continental arc in the Alborz ranges, N-Iran, 2012, **Lithos**, 148, 98–111.

AZIZI, H., HADAD, S., STERN, R., ASAHARA, Y. Age, geochemistry, and emplacement of the ~40-Ma Baneh granite–appinite complex in a transpressional tectonic regime, Zagros suture zone, northwest Iran. 2018. **International Geology Review**, DOI: 10.1080/00206814.2017.1422394

COX, K. G., BELL, J. D. & PANKHURST, R. J. **The Interpretation Igneous rocks**. London: George Allen & Unwin, 1979.

DABIRI, Rahim; AKBARI-MOGADDAM, Mohsen; GHAFFARI, Mitra. Geochemical evolution and petrogenesis of the eocene Kashmar granitoid rocks, NE Iran: implications for fractional crystallization and crustal contamination processes, **Iranian Journal of Earth Sciences**, 10(1) pp 68-77. 2018.

GLASSER, N.; BENNET. R.M.; HUDDART, D. Distribution of glaciofluvial sediment within and on the surface of a high arctic valley glacier: Marthabreen, Svalbardh. 1999. **Journal of Earth surface processes and landforms.** Vol. 24., pp. 303-318.

GLAZNER, A. F.; W. USSLER III. Crustal extension, crustal density, and the evolution of Cenozoic magmatism in the Basin and Range of the western United States, 1989. **J. Geophys. Res.**, 94, 7952–7960, doi:10.1029/ JB094iB06p07952.

GREEN, L. Influence of slab thermal structure on basalt source regions and melting conditions: REE and HFSE constraints from the Garibaldi volcanic belt, northern Cascadia subduction system. 2006. **Journal of Lithos**, 87, 23– 49pp.

GUEST, B.; GUEST, A.; AXEN, G. Late Tertiary tectonic evolution of northern Iran: A case for simple crustal folding. 2007. **Journal of Global and Planetary Change** 58: 435-453.

HUMPHREYS, E., E. HESSLER, K. DUEKER, G. L. FARMER, E. ERSLEV, AND T. ATWATER. How Laramide-age hydration of North American lithosphere by the Farallon slab controlled subsequent activity in the western United States. 2003. **Int. Geol. Rev.**, 45, 575–595, DOI:10.2747/0020- 6814.45.7.575.

IRVINE, T. N. & BARAGAR, W. R. A. A Guide to the chemical classification of the common Volcanic Rocks. 1971. **Canadian Journal of Earth Science** 8: 523-548.

PEARCE J.A. Role of the sub-continental lithosphere in magma gensis at activevcontinental margins. In: HAWKESWORTH C. J.; NORRY M. J. (eds.). **Continental basalts and Mantle Xenoliths.** Shiva ,Natwich, 1983, p. 230–249.

PLANK, T.; C. H. LANGMUIR. An evaluation of the global variations in the major element chemistry of arc basalts. 1988. **Earth Planet. Sci. Lett.**, 90, 349–370, DOI:10.1016/0012-821X(88)90135-5.

STÖCKLIN, J. Structural history and tectonics of Iran: A review. 1968. **American Association of Petroleum Geologists**, v.52, p. 1229–1258.

SUN, S. S.; MCDONOUGH, W. F. Chemical and isotopic systematics of oceanic basalts: implications for mantle composition and processes" In: SAUNDERS, A.D., NORRY, M.J. (Eds.), Magmatism in the Ocean Basins. 1989. **Geol Soc Spec Publ.**, vol. 42, p. 313-345.

TAPPA, M.J., COLEMAN, D.S., MILLS, R.D., AND SAMPERTON, K. M. The plutonic record of a silicic ignimbrite from the Latir volcanic field, New Mexico. 2011. **Geochemistry, Geophysics, Geosystems**, v. 12, no. 10, Q10011, DOI: 10.1029/2011GC003700.

TEMIZEL, I; ARSLAN, M. Petrology and geochemistry of Tertiary volcanic rocks from the-Ikizce (Ordu) area, NE Turkey: Implications for the evolution of the eastern Pontide paleo-magmatic arc. 2008. **Journal Of Asian Earth Science**, 31, pp. 439-463.

WHITE, R. S.; MCKENZIE, D. Mantle plumes and flood basalts. 1995. **J Geophys Res.**, Vol. 100, p. 17543-17585.

YAXLEY, G. M. Experimental study of the phase and melting relations of homogeneous basalt+peridotite mixtures and implications for the petrogenesis of flood basalts. 2000. **Contrib Mineral Petr.**, Vol. 139, p. 326-338.

YAZDI, A.; SHAHHOSINI, E.; DABIRI, R.; ABEDZADEH, H. Magmatic Differentiation Evidences And Source Characteristics Using Mineral Chemistry In The Torud Intrusion (Northern Iran). 2019. **Revista GeoAraguaia**, 9(2): 6-21.

ZANCHI, A., BERRA, F., MATTEI, M., GHASSEMI, M. R.; SABOURI, J. Inversion tectonics in Central Iran, 2006. **Journal of Structural Geology** 28: 2023-2037.

ZENG, G., CHEN, L., XU, X., JIANG, SH.; HOFMANN, A. Carbonated mantle sources for Cenozoic intra-plate alkaline basalts in Shandong, North China. 2010. **Chem. Geol.**, Vol. 273, PP. 35-45.

ZONENSHAIN, L. P.; LEPICHON, X. Deep basins of black sea and Caspian Sea as remnants of Mesozoic back-arc basin. 1986. **Tectonophysics**. 123: 181-211.